Forecasting River Uruguay flow using rainfall forecasts from a regional weather-prediction model

Walter Collischonn[a,*], Reinaldo Haas[b], Ivanilto Andreolli[a], Carlos Eduardo Morelli Tucci[a]

[a]*Instituto de Pesquisas Hidráulicas, Universidade Federal do Rio Grande do Sul, Av. Bento Gonçalves, 9500, Caixa Postal 15029, CEP 91501-970, Porto Alegre, RS, Brazil*
[b]*Departamento de Engenharia Sanitária e Ambiental, Universidade Federal de Santa Catarina, Caixa Postal 476, Campus Universitário Trindade, CEP 88010-970, Florianópolis, SC, Brazil*

Abstract

The use of quantitative rainfall forecasts as input to a rainfall-runoff model, thereby extending the lead-time of flow forecasts, is relatively new. This paper presents results from a study in which real-time river flow forecasts were calculated for the River Uruguay basin lying within southern Brazil, using a method based on observed rainfall, quantitative forecasts of rainfall given by a regional numerical weather-prediction model, and rainfall-runoff simulation by a distributed hydrological model. The performance of discharge forecasts was evaluated over a continuous 167-day period and from one selected flood event, using rainfall forecasts at three spatial resolutions. The performance of these forecasts was also compared with that of forecasts obtained (a) by assuming that no further rain would fall, and (b) by assuming that rainfall forecasts were equal to the rainfall actually recorded, this representing a surrogate for 'perfect' rainfall forecasts. The results show that for the basin considered, there is plenty of scope for improving usefulness of rainfall forecasts.
© 2004 Elsevier B.V. All rights reserved.

1. Introduction

High-quality and timely forecasts of inflows into reservoirs used to generate hydropower result in improved management of water resources, increasing the benefits from power generation and reducing risks associated with spillway operation. Information obtained by hydrological forecasts gives valuable support for decision-making, bringing benefits from reduction in flood damage, increased dam safety, and greater efficiency in power generation, whilst some environmental problems associated with dams are diminished (Yeh et al., 1982; NHWC, 2002).

This paper follows the convention that flow forecasts with lead-times from a few hours to 2 or 3 days are termed short-term forecasts, to distinguish them from seasonal forecasts that extend for a few

---

* Corresponding author.
E-mail address: cllschnn@vortex.ufrgs.br (W. Collischonn).

months into the future. Short-term forecasts may be obtained either by channel-routing methods or by simulating processes that transform rainfall into runoff; in many applications, forecasts based on channel-routing are preferred because of their simplicity. Forecasting based on rainfall-runoff transformation is more complex since extensive rainfall data and detailed information of basin topography, vegetation and soil characteristics are also required for the description of hydrological processes. Nevertheless, forecasting by rainfall-runoff models is essential whenever the forecast lead-time is significantly longer than the time taken to route flow along the river channel (Lettenmaier and Wood, 1993).

When the forecast lead-time is greater than the sum of basin concentration time and flood propagation time for the channel system, rainfall observations alone are not sufficient for forecasting purposes, since rain that has been transformed into runoff passes the basin outfall before expiry of the lead-time. Some estimate of future rainfall is therefore required if flow forecasts are to be issued up to the end of the lead-time period; a lower limit to the forecast flow is given by setting all future rainfall equal to zero, but it is clearly more desirable to obtain quantitative precipitation forecasts (QPFs) provided that these are sufficiently accurate. Increasingly, QPFs are being supplied by numerical weather-prediction models (NWPs).

The use of QPFs as input to extend the useful lead-time of forecasts from rainfall-runoff models is relatively undeveloped, possibly because QPFs in the past have shown low reliability. Rainfall is still one of the most difficult variables to predict from NWP models, but recent results suggest that progress is being achieved towards bringing QPFs to the stage of operational usefulness for hydrological applications (Hollingsworth, 2003; Collier and Krzysztofowicz, 2000; Damrath et al., 2000; Golding, 2000; Mao et al., 2000; McBride and Ebert, 2000; Mullen and Buizza, 2001). However, although the combined use of hydrological rainfall-runoff models and NWP models has been tested by several authors (Yu et al., 1999; Ibbitt et al., 2000; Anderson et al., 2002; Jasper et al., 2002; Koussis et al., 2003) the focus has concentrated mainly on forecasting a few selected flood events. This paper extends the results of these authors by describing a methodology and some results from forecasting flow in the River Uruguay at

the Machadinho hydroelectric reservoir, using observed rainfall, QPFs obtained from a NWP model, and a distributed rainfall-runoff model, with flow forecasts evaluated retroactively for one flood event and for a continuous period of 167 days.

2. Study site and forecasting methodology

2.1. The Uruguay river basin at Machadinho

The River Uruguay is one of the main tributaries of the la Plata river basin, the second largest in South America. Its headwaters lie entirely within Brazilian territory, where two hydroelectric power dams were constructed between 1999 and 2000. The area modelled in the present paper is upstream of Machadinho, the first dam in the downstream direction, with drainage area 32,000 km^2. A short distance upstream of this dam, two rivers—the Canoas and Pelotas—join to form the River Uruguay proper. Annual mean temperature is in the range of 15.2–14.3 °C for two settlements at an altitude of about 950 m, although over large areas the altitude rises to 1800 m. The entire basin lies on basalt covered by shallow clay soils with low infiltration capacity. Mean annual rainfall is between 1300 and 1500 mm. Rainfall is lower in the east and is usually well distributed over the year; dry and wet periods often alternate rapidly, resulting in a highly erratic and unpredictable river flow regime. Rapid surface flows dominate the hydrograph (Fig. 2), and discharge into the Machadinho reservoir can increase from below 1000 m^3 s^{-1} to more than 14,000 m^3 s^{-1} in 2 days, as shown below. Large areas of the basin are under grassland, some of which is natural. Clumps of forest are relatively common in areas with steeper gradient but urban and cultivated areas are rare.

Compared with much of Brazil, this part of the Uruguay basin is relatively well covered with rain gauges. There are 36 in all, 18 of which are automatic, which telemeter measurements in real time as seen in Fig. 1. To make best use of all available data, daily rainfall totals recorded at manual gauges were transformed into hourly data by using the time distribution of the nearest automatic rain gauges.

There are also two automatic stream gauging stations, one on the river Canoas, at the point where
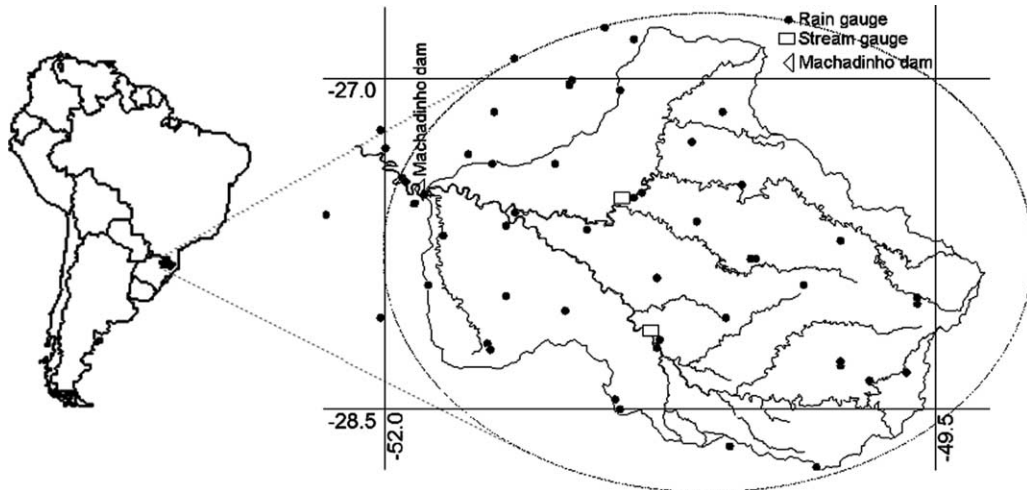
Fig. 1. Location of the study region, main features of the basin and gauging stations.

the drainage area is 10,250 km^2, one on the river Pelotas (8400 km^2). Stage and rain gauges transmit level and rainfall at 1-h intervals.

2.2. The hydrological model

Collischonn and Tucci (2001) have described a distributed hydrological model for large drainage basins, using information from satellite images, digital elevation models and digitized maps of land use, vegetation cover, relief and soils. The model is similar to the LARSIM (Bremicker, 1998) and VIC-2L (Wood et al., 1992; Liang et al., 1994; Nijssem et al., 1997) models. The basin area is divided into square cells, each of which is further sub-divided into blocks representing soil-type, land use and vegetation cover. The original time-step of 1 day has been modified to allow smaller time-steps, and hourly steps were used in the present work.

Soil water balance is computed independently for each block of each cell, considering only one soil layer. The model has components representing canopy interception, evapotranspiration, infiltration, surface runoff, sub-surface flow, baseflow and soil water storage. Rainfall values are interpolated spatially and at each time-step, to give an estimate at the center of each grid cell, using the inverse-distance-squared interpolation method. Flow generated within each cell is routed to the stream network using three linear reservoirs (baseflow, sub-surface

flow, and surface flow). Streamflow is propagated through the river network using the Muskingum–Cunge method.

The Uruguay river basin above Machadinho was divided into 291 cells, 0.1° wide. Vegetation cover and land use were classified based on LANDSAT TM7 images, giving five classes: pasture, forest, agriculture and water. The model was calibrated using rainfall and runoff data from September 2001 to May 2003. During the first month of this period, the Uruguay river basin experienced a large flood, which peaked 5300, 2600 and 13,700 m^3 s^{-1} in the rivers Pelotas, Canoas and Uruguay, respectively. (In the case of the rivers Canoas and Pelotas, these peak flows were obtained from flow gauges; in the case of Uruguay flow into Machadinho, the inflow was estimated by water budget). In this flood event, some rain gauges in the southern part of the basin recorded almost 200 mm rainfall in 24 h. A long dry period followed the large flood of September 2001, as can be seen from Fig. 2. Some minor floods occurred in late 2002, but 2003 was also dry.

The model was calibrated using the multi-objective automatic MOCOM-UA algorithm (Yapo et al., 1998). This technique allows the optimization of two or more objective functions at the same time, what is useful in the case of distributed models since results can be compared at more than one point over the basin. The Nash–Sutcliffe coefficients (denoted by NS: see Eq. (1)) at the three flow gauges were selected
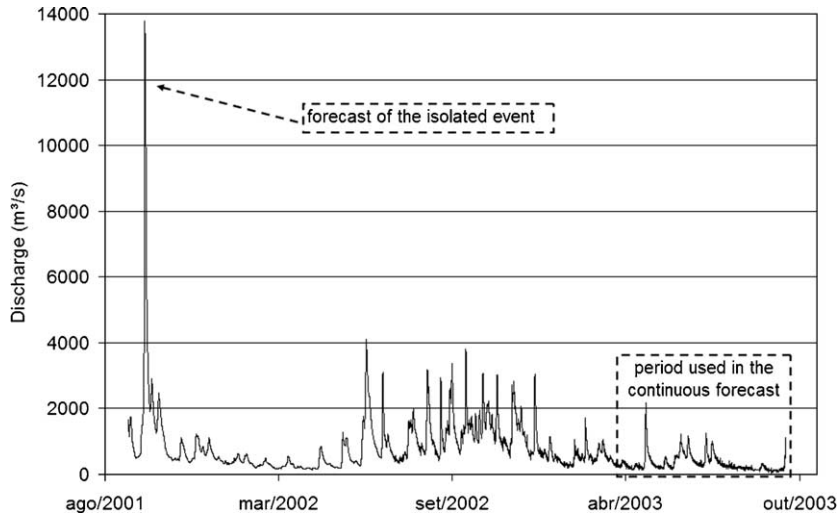
Fig. 2. Observed hydrograph at Machadinho Reservoir from September 2001 to October 2003.

as the objective functions

$$NS = 1 - \frac{\sum (Q_{obs}(t) - Q_{cal}(t))^2}{\sum (Q_{obs}(t) - \bar{Q}_{obs})^2} \qquad (1)$$

where $Q_{obs}(t)$, $Q_{calc}(t)$ are the observed and calculated discharges at time-step t.

Calibration was assessed using the final values of the objective functions and on the fit between observed and calculated hydrographs. The model efficiency NS was 0.89 at Machadinho, with a relative volume error of 3.2%. Observed and calculated hydrographs of the River Uruguay during the austral winter of 2002 are shown in Fig. 3. Most of the peak
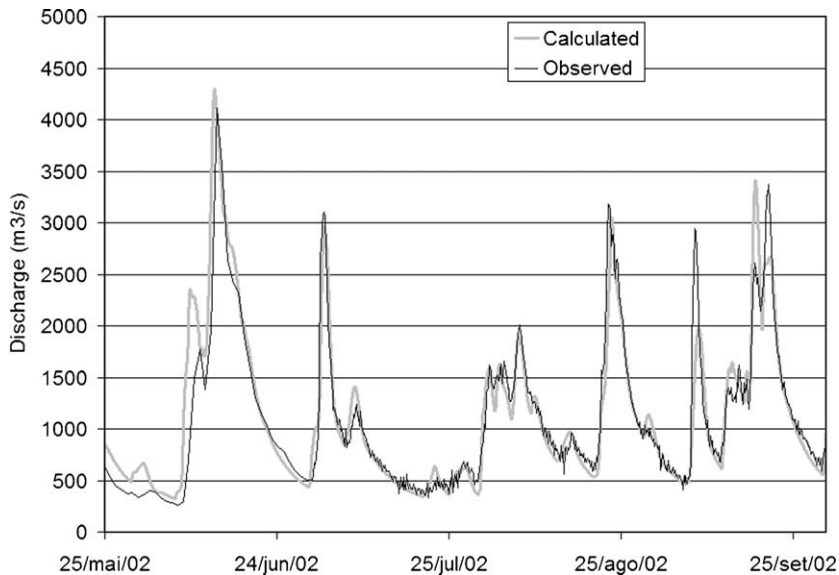

Fig. 3. Calculated and observed hydrographs for part of the calibration period (May–September 2002).

flows are well reproduced; the noise ripples during the observed hydrograph recession arise because inflows to Machadinho were estimated by water budget.

3. Updating procedure

Real time flow forecasts can be improved by continuously comparing forecast results to observations and by changing values of some internal variables or parameters to reduce the differences (Serban and Askew, 1991). This updating procedure is more difficult when the forecasting model has a large number of state variables, as is the case for a distributed hydrological model, but the problem can be simplified by limiting the number of state variables that are updated. In this paper, the updating procedure was based on the comparison between observed and calculated flows at the two gauges on the Pelotas and Canoas rivers, where the areas drained are 8400 and 10,250 km^2, respectively. Almost half of the whole Machadinho drainage area lies above these two gauges.

Observed discharges at the two gauges were divided by discharge calculated with zero hour antecedence, i.e. discharge calculated using only observed rainfall, giving an updating correction factor denoted by FCA in Eq. (2). The discharge variable in each cell upstream of the gauges was then updated according to Eq. (3), using the correction FCA and the relation between drainage area at the cell and at the gauge. This means that the calculated discharge corrections were weighted according to the reliability of the information at the streamgauge. At the cell where the streamgauge is located, observed flows were used in place of calculated. For cells close to the streamgauge, this scheme assumes that flow recorded at the streamgauge is virtually correct. For cells far upstream of the gauge, calculated flows are assumed to be more reliable, and corrections are damped out following Eq. (3):

$$\text{FCA}_k = \frac{Q_{\text{obs}}}{Q_{\text{calc}}} \qquad (2)$$

$$Q_{\text{up}_{i,k}} = \text{FCA}_k \times Q \times \left(\frac{A_i}{A_k}\right) + Q_{\text{calc}_i}\left(1 - \frac{A_i}{A_k}\right) \qquad (3)$$

In (2) and (3), k is the gauge considered (1 for Pelotas and 2 for Canoas); Q_{obs} is the observed discharge and Q_{calc} is the calculated discharge; $Q_{\text{up}_{i,k}}$ is the updated value of discharge at cell i, located upstream of gauge k; A_i is the drainage area upstream of the i cell and A_k is the drainage area upstream of gauge k.

The updating procedure described above refers to the river discharge variable. A similar updating procedure was adopted to correct volumes in groundwater storage. Each cell of the model has three linear reservoirs that represent the retention and delay of water subsequently released as surface, subsurface and groundwater flow. Outflow from these reservoirs in each cell becomes inflow to the river network where it is routed using the Muskingun–Cunge method (Collischonn and Tucci, 2001). During long dry periods, the greater part of flow comes from groundwater storage. The model maintains a continuous record of the fraction of flow in the drainage network that comes from surface, sub-surface and groundwater. Groundwater storage in each cell upstream of streamgauge k is updated using the same correction factor (FCA) used for river flow, but corrections are weighted by the fraction of river flow that is from groundwater origin (PB_i), according to (4):

$$\text{VB}_{\text{up}_i} = \text{FCA}_k \times \text{VB}_i \times (\text{PB}_i) + \text{VB}_i(1 - \text{PB}_i) \qquad (4)$$

where VB_{up_i} is the updated storage in the groundwater reservoir of cell i; VB_i is the calculated storage at cell i and PB_i is the fraction of river flow at cell i that originated from groundwater.

Thus, the discharge recorded at two sites was used to update state variables distributed over half of the basin. As a consequence, the initial conditions taken by the model at the start of each forecasting cycle were fairly good, although the updating procedure could not be thoroughly tested because streamflow records were too short. It is believed that with more runoff data, especially at the basin outlet, forecasts for short-range forecasts (0–12 h) would be considerably improved.

4. Quantitative precipitation forecasts

Since 1995, most research on meteorological models and operational weather forecasts in Brazil

has been the responsibility of the Brazilian Center for Weather and Climate Prediction (CPTEC) of the National Space Research Institute (INPE). Weather forecasts using regional models are also issued by the National Institute of Meteorology (INMET) and by several research centres and universities. In this paper, weather forecasts were obtained from the Federal University of Santa Catarina State (Haas, 2002), where the Advanced Regional Prediction System (ARPS, Xue et al., 2000, 2001) has been in use since 2002. ARPS is a three-dimensional, non-hydrostatic model system designed for the explicit representation of convective storms and weather systems at other scales. The variables predicted include Cartesian wind components, potential temperature and pressure, sub-grid-scale turbulent kinetic energy, mixing ratios for water vapor, cloud water, rainwater, cloud ice, snow and graupel/hail. Several options exist for cloud microphysics and cumulus parameterization (Xue et al., 2000).

In operation, ARPS uses three nested domains centered over South Brazil. The 103×63 node outer grid has a spatial resolution of 40 km (ARPS-40) and spans the area between 85 to 35°W, and 15 to 48°S. Boundary conditions for this simulation are obtained from the NCEP AVN global model. The 123×123 node intermediary grid has a spatial resolution of 12 km (ARPS-12) and spans the area from Uruguay (34°S) to the states of Minas Gerais and Mato Grosso do Sul (22°S), and from middle Paraguay (60°W) to part of the South Brazilian coastal area of the Atlantic Ocean (46°W). Finally the 143×123 node grid has a resolution of 4 km (ARPS-4) and spans a very limited area that covers only the State of Santa Catarina and parts of the neighbouring States of Rio Grande do Sul (to the South) and Paraná (to North): that is, 48–54°W and 26–30°S. In the vertical direction, the domain is divided into 35 levels, which are 20 m high at the surface to 500 m high at the top of the model domain, at 9 km. Operational forecasts are initiated twice a day, at 00:00 Z and 12:00 Z UTC (Coordinated Universal Time), corresponding to 21:00 and 09:00 local time. Runs of the ARPS model on the 40, 12 and 4 km domains have lead-times of 60, 50, and 36 h, respectively. Two important features of the model relating to QPF, are the use of Goddard Ice Microphysical scheme (Lin et al., 1983;

Tao and Simpson, 1993) and Kain and Fritsch cumulus parameterization (Kain and Fritsch, 1993).

Continuous storage of rainfall forecasts of the ARPS model began on 25 May 2003, and these were analyzed up to 10 October 2003 when the work reported in this paper was completed. Prior to this period, very few rainfall forecasts had been retained. The flood event of September–October 2001 was used to supplement the continuous period 25 May–10 October 2003 (167 days) used in the test reported here.

5. Flow forecasting procedure

In the flow-forecasting procedure, observed and forecast rainfall were used as input to the distributed rainfall-runoff model. The hydrological model was run in continuous simulation mode, using observed rainfall data up to the time of forecast start (t_0). From this time up to the flow forecast lead-time, the model was used with five alternative rainfall forecasts: (a) zero rainfall; (b) ARPS-40 km forecast rainfall; (c) ARPS-12 km forecast rainfall; (d) ARPS-4 km forecast rainfall; and (e) observed rainfall over the lead-time period, which was considered a surrogate of a perfect rainfall forecast. Fig. 4 illustrates this method with two alternative rainfall forecasts: zero rainfall and one NWP model forecast rainfall.

When forecasting over the continuous period, time-steps of 1 h were used. A new flow-forecasting cycle was initiated each hour, and ended at the completion of the lead-time. Values of the variables of the hydrological model were then changed for the values calculated at t_0, and the model was run for one time-step (hour) using observed rainfall, thus initiating a new forecast at time $t_0 + 1$, and so on. River flow and groundwater storage were also updated at each t_0.

6. Results from the 2001 flood event

The forecasting methodology was first tested using the September/October 2001 flood event. The return period of this flood was close to 100 years, and since it was the first major flood experienced by the newly built dam at Machadinho, there was much concern for its safety.
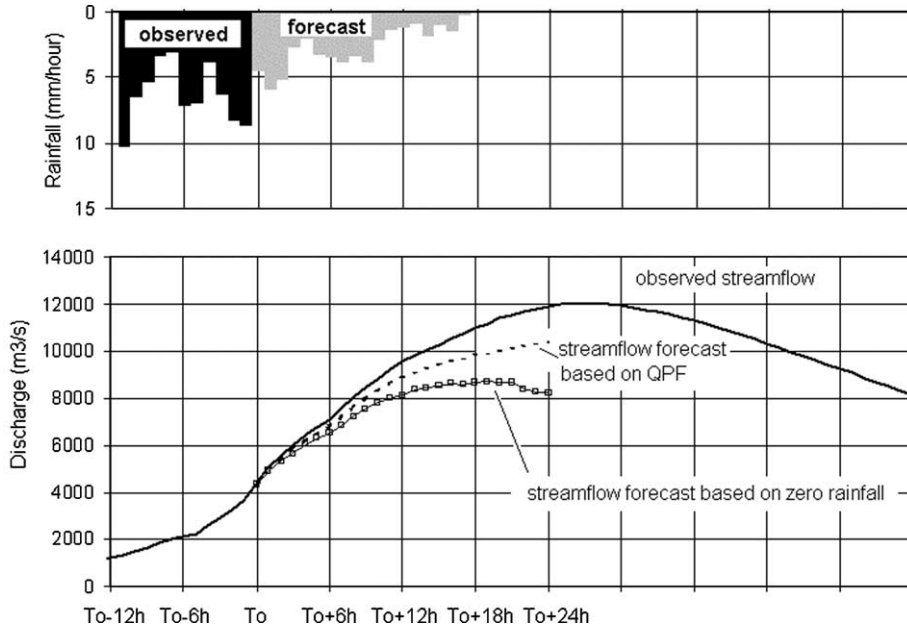
Fig. 4. Scheme of flow forecast procedure using observed rainfall data up to the starting time of the forecasts, and zero rainfall or forecast rainfall up to the lead-time.

Water-level in the reservoir was only recorded once a day at the time of this flood, so the observed hydrograph, derived by reservoir water budget, has a very low time resolution. Fig. 5 show results for the 2001 flood. Fig. 5a shows forecasts issued at 07:00 on 30 September, using rainfall forecasts initiated at 21:00 on 29 September, and using observed rainfall data up to 07:00. At this time, the basin has still not received much rain, and the streamflow forecast based on the zero rain forecast shows a recession. Streamflow forecasts based on NWP show better performances, although all three versions of the ARPS model seem to underestimate rainfall for this event. Flow forecasts based on rainfall forecasts at the 40 km resolution of the ARPS model (ARPS-40) correctly predict rising flows, but peak discharge is estimated at less than 3000 $m^3 s^{-1}$: far less than the observed peak discharge of close to 14,000 $m^3 s^{-1}$. The ARPS-12 model performed a little better, giving forecasts of peak discharge near 5000 $m^3 s^{-1}$ more than 24 h in advance. Although the forecast discharge is still underestimated, under operational conditions it would signal the occurrence of a relatively high flood during the coming hours,

alerting to the possible need for damage-prevention measures.

As shown in Fig. 5a, discharge forecasts based on the 4 km resolution ARPS-4 model seem to be better than the others. However, ARPS-4 forecasts were only possible for a lead-time of 24 h, too short for forecasts up to the hydrograph peak. Fig. 5b shows discharge forecasts performed at midnight 30 September, with the same rainfall forecast runs of Fig. 5a, and observed rainfall data up to midnight. At this time, a great deal of rain had fallen, and flow entering Machadinho showed that peak discharge would rise well above 5000 $m^3 s^{-1}$, as forecast at 07:00. Even the forecast of incoming flow assuming no further rainfall showed that the hydrograph would rise for the next 20 h, with a peak of about 12,000 $m^3 s^{-1}$; this forecast, interpreted as the lower limit of an uncertainty range, would be very useful for dam operation purposes. Fig. 5b also shows that forecasts based on all three ARPS models with their different resolutions gave estimates of peak discharges well in excess of 12,000 $m^3 s^{-1}$, even approaching 15,000 $m^3 s^{-1}$ in the case of the ARPS-12 model.

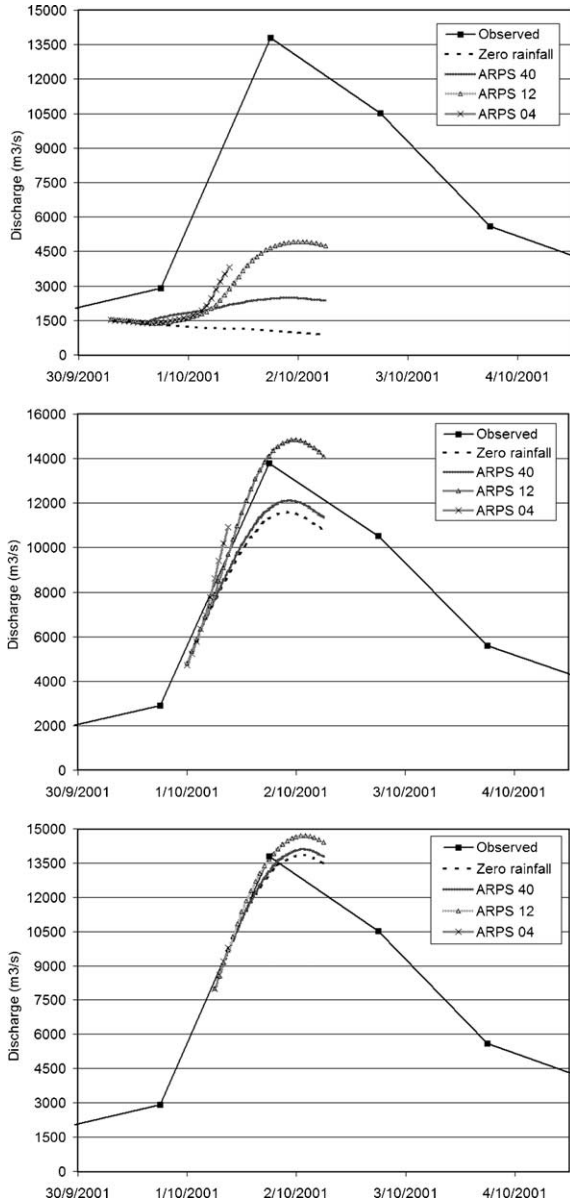Finally, forecasts initiated at 06:00 on 1 October are very similar for the different rainfall forecasts

Fig. 5. Incoming flows to the Machadinho reservoir: (a) forecasts beginning at $t_0 = 07{:}00$ h of 30 September 2001; (b) forecasts beginning at $t_0 = 00{:}00$ h of 1 October 2001; forecasts beginning at $t_0 = 06{:}00$ h of 1 October 2001.

(Fig. 5c). As can be seen, even the zero rainfall forecasts gave good forecasts of incoming flow to the reservoir. Although the timing of the observed peak flow is largely uncertain, it was estimated that peak incoming flows would occur in the early hours of

1 September, so that the good results in Fig. 5c could have been obtained 10 h in advance of the observed peak flows.

Results of this single event analysis suggest that better QPF can be obtained by increasing the spatial resolution of the NWP model. This may be related to the convective origin of most of the heavy rain falling during this flood event, and to the better representation of relief in high-resolution NWP models, due to the strong influence of relief on rainfall.

7. Results from the period of continuous forecasting

Weather forecast files were stored continuously from April to October 2003. Streamflow forecasts were performed a posteriori for this period, as if under operational conditions. This means that (1) the hydrological model was calibrated with observed data of a past period; (2) observed rainfall was used only up to t_0; (3) observed discharges at gauging stations of the rivers Canoas and Pelotas were used to update the model at time t_0; and (4) only QPFs that would be available at t_0 were used (due to the time needed to calculate them, this means that the QPFs used were those from NWP runs initiated up to 10 h earlier).

Flow forecasts were initiated at each hour, and extended 48 h into the future, except for those derived from ARPS-4 rainfall forecasts, which extended for only 15 h. This means that the hourly observed hydrograph could be compared with 48 (15) forecast hydrographs, according to the lead-time. Comparison was simplified by using statistical performance criteria of the forecasts. The first of these criteria is the Nash–Sutcliffe coefficient given in (1). The second, the coefficient of persistence CP (Kitanidis and Bras, 1980), which compares the discharge forecast by the model with a 'no model forecast', in which the latest observed discharge ($Q_{O_{t_0}}$) is held constant as in (5):

$$\mathrm{CP}_\tau = 1 - \frac{\sum_{i=1}^n (Q_{P_{t+\tau}} - Q_{O_{t+\tau}})^2}{\sum_{i=1}^n (Q_{O_{t+\tau}} - Q_{O_t})^2} \tag{5}$$

where t is the time at which the forecast of discharge is initiated; τ is the forecast lead-time; $Q_{P_{t+\tau}}$ is the discharge forecast at time $t+\tau$; $Q_{O_{t+\tau}}$
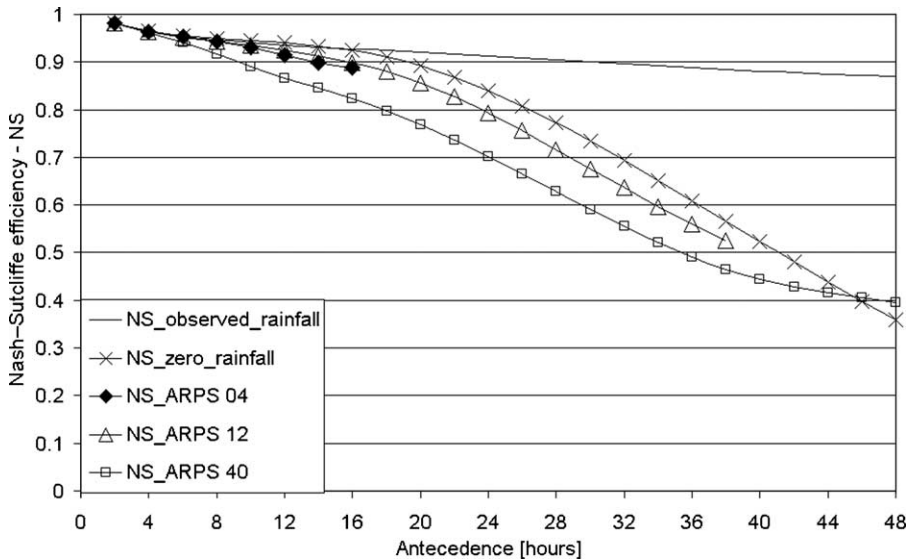
Fig. 6. Nash–Sutcliffe coefficient of performance of discharge forecasts, based on different rainfall forecasting methods: zero rainfall; observed rainfall; and ARPS forecasts at 4, 12, and 40 km resolution. Symbols are explained in the text.

is the discharge observed at time $t+\tau$; Q_{O_t} is the observed discharge at time t; CP_τ is the coefficient of persistence for discharge forecasts with lead-time τ; and n is the number of time intervals.

Results for NS and CP are plotted against lead-time, or antecedence of the forecasts, in Figs. 6 and 7. The Nash–Sutcliffe coefficients of five forecasting methods are plotted in Fig. 6, according to the origin

of rainfall data that was used for the time between t and $t+\tau$: zero rainfall (line with crosses); observed rainfall (line); and three types of forecast rainfall by the different resolution ARPS models (4, 12 and 40 km—line with full diamonds, triangles and squares, respectively). The NS coefficients have very high values for short antecedence times, due to the updating procedure used. The NS for forecasts
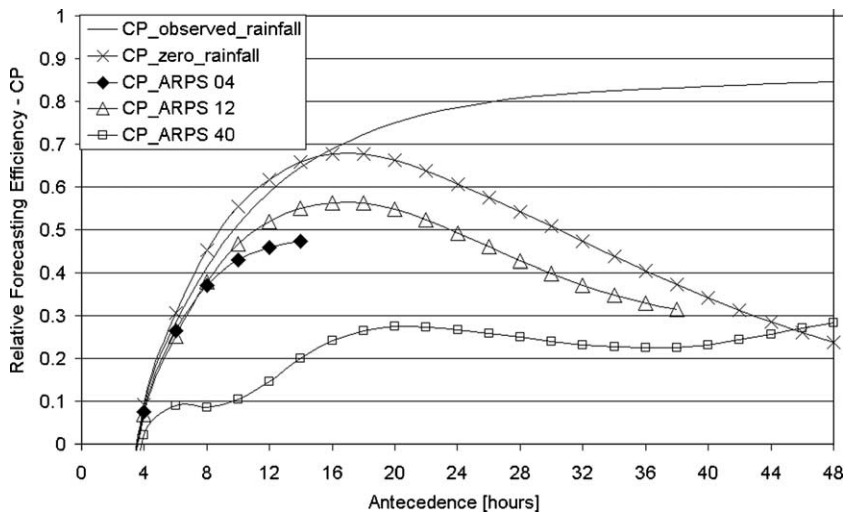

Fig. 7. Coefficient or persistence of discharge forecasts based on different rainfall forecasting methods: zero rainfall; observed rainfall; and ARPS forecasts in 4, 12, and 40 km resolution. Symbols are explained in the text.

based on observed rainfall remain above 0.9 for up to 24 h antecedence, and are still high up to 48 h. Discharge forecasts assuming zero rainfall cannot be distinguished from those based on observed rainfall up to 16 h in advance, but begin to show decreased efficiency beyond this threshold. Surprisingly, all forecasts of discharge based on forecast rainfall show poorer performances than those of the zero-rainfall method. At antecedence times of 44–48 h, however, the forecasts based on the ARPS-40 km rainfall forecasts perform better than the zero-rainfall method.

Fig. 7 gives corresponding results for the persistence coefficient CP. Below 4 h, there is apparently no advantage in using any of the discharge forecasts based on rainfall-runoff simulation (values of CP are negative and are not shown). Forecasts based on zero rainfall and ARPS-12 rainfall forecasts perform well up to 16 h in advance, but performance falls off thereafter. These results agree with those obtained for the single 2001 flood event, and it can be concluded that, for the Uruguay basin under study, good forecasts of discharge can be obtained up to a lead-time between 10 and 16 h, using only observed rainfall. Forecasts based on ARPS-4 appear to show similar performance, but are limited in that forecasts of rainfall, and hence forecasts of discharge, are only possible up to 15 h in advance. Forecasts based on ARPS-40 forecasts have a distinct behavior, showing a relative forecasting efficiency (CP) which increases very slowly.

It is surprising that, in so many of the antecedence times, forecasts of discharge derived from the QPF forecasts of ARPS models perform less well than those obtained assuming zero rainfall. As Fig. 7 shows, only at antecedence times beyond 46 h does there seem to be any advantage in using ARPS-40 QPFs, instead of ignoring the future rainfall.

The relative performance of streamflow forecasts based on observed rainfall, as a surrogate of 'perfect QPFs' is also shown in Fig. 7. For lead-times up to 16 h, there is no advantage in using observed rainfall instead of zero rainfall, but from 16 h onwards the performance of flow forecasts based on observed rainfall continues to increase, while the performance of forecasts obtained by assuming zero rainfall rapidly decreases. It is clear from this figure that there is room for improvements in QPFs, especially for lead times in the 16–48 h interval. The poor results during this period of continuous forecasting were unexpected,

since during the first part of the continuous period (April–June: not shown in this paper) discharge forecasts based on QPFs performed better than those based on zero rainfall. The explanation may lie in the fact that the results reported in this paper were from a very dry test period, what would favour discharge forecasts based on persistence and on zero rainfall forecasts. In such a dry period, a few storm events with rainfall overestimated by the NWP models would adversely affect forecasting performance. It is expected that in periods marked by the frequent and rapid floods that are typical of the basin, forecasts based on QPFs would perform better.

Another possible explanation for these poor results is the timing error of the rainfall forecasts. We observed that the NWP model gives late rainfall forecasts, possibly due to poor initial conditions used for each forecasting run. In our forecasting methodology, these late forecasts are used in addition to the rainfall observations, resulting in rainfall events used as input to the rainfall-runoff hydrological model that are longer than those observed, and total rainfall per event that is larger than observed. We think that due to this timing error the hydrographs forecast using QPFs may be overestimated, particularly immediately after the peak flow. Preliminary tests not described in these paper show that better results may be obtained by simply shifting the QPFs 10 h earlier. Although this shift could not be done in operational forecasts, the results indicate that the available QPFs should be better explored by understanding the uncertainty associated to its timing and position errors.

8. Conclusions

This paper has described an application of short-term flow-forecasting, using a procedure based on quantitative rainfall forecasts, rainfall observations, and a rainfall-runoff simulation model. The procedure was tested for a large flood event and over a continuous period of 167 days, as if under operational conditions. The area studied was the River Uruguay basin up to the Machadinho dam and reservoir, located in an upland region of southern Brazil. Observed and forecast rainfall data were used to drive a distributed hydrological model, giving reservoir inflow forecasts up to 48 h in advance. Rainfall

forecasts were obtained from the ARPS model run in three nested domains, with spatial resolutions of 40, 12, and 4 km. This model has been running operationally since early 2003 at the Federal University of the State of Santa Catarina.

Results obtained for the large flood of year 2001 showed that the rainfall forecasts were generally under-predicted during this event. However, very good peak inflow forecasts could be made with more than 10 h in advance, and flow forecasts based on quantitative precipitation forecasts performed better than the ones obtained assuming zero rainfall in future hours. Results obtained for the continuous period showed that discharge forecasts based on rainfall forecasts were not better than those made using zero rainfall forecasts, suggesting that it should be better to ignore future rainfall than to use QPFs. This result was unexpected, but the explanation may be that the continuous period was very dry, showing few flood pulses. Different results are expected for wetter periods. Another explanation to this unexpected result may be that timing errors of the rainfall forecasts would result in overestimation of the streamflow after the peak of the hydrograph.

The flow forecasting methodology based on the hydrologic simulation model shows very useful results up to 10 or 16 h in advance. This threshold is related to the short response time of the basin, although its area extends over 32,000 km^2. Inflow to the Machadinho reservoir on the River Uruguay is dominated by rainfall that has already fallen up to 16 h in advance, and can therefore be forecast very well even if zero rainfall is assumed in the immediate future. Beyond 16 h, the performance of flow forecasts based on zero precipitation forecasts decreases rapidly.

The performance of discharge forecasts obtained by using observed rainfall, as a surrogate for perfect rainfall forecasts, was also investigated. In this case the performance was quite high even for antecedences well beyond 16 h. This result indicates that there is further benefit to be derived by improving quantitative precipitation forecasts over the range 16–48 h in this basin, assuming the same basis for rainfall-runoff modelling.

Acknowledgements

References

Anderson, M.L., Chen, Z.Q., Kavvas, M., Feldman, A., 2002. Coupling HEC-HMS with atmospheric models for prediction of watershed runoff. Journal of Hydrologic Engineering 7, 312–318.

Bremicker, M., 1998. Aufbau eines Wasserhaushaltsmodells für das Weser und das Ostsee Einzugsgebiet als Baustein eines Atmosphären-Hydrologie-Modells. Dissertation Doktorgrad, Geowissenschaftlicher Fakultät der Albert-Ludwigs-Universität. Freiburg. Juli.

Collier, C.G., Krzysztofowicz, R., 2000. Quantitative precipitation forecasting. Journal of Hydrology 239, 1–2.

Collischonn, W., Tucci, C.E.M., 2001. Hydrologic simulation of large basins (in Portuguese). Revista Brasileira de Recursos Hídricos 6 (1).

Damrath, U., Doms, G., Frühwald, D., Heise, E., Richter, B., Steppeler, J., 2000. Operational quantitative precipitation forecasting at the German Weather Service. Journal of Hydroloy 239, 260–285.

Golding, B.W., 2000. Quantitative precipitation forecasting in the UK. Journal of Hydrology 239, 286–305.

Haas, R. 2002. Simulation of orographic precipitation associated to an extra tropical cyclone (in Portuguese). PhD Thesis IAG USP, Brazil.

Hollingsworth, A., 2003. Improvements in the skill of numerical weather prediction with global models. Bulletin World Meteorological Organization 52, 33–39 (OMM. publ. no. 1).

Ibbitt, R.P., Henderson, R.D., Copeland, J., Wratt, D.S., 2000. Simulating mountain runoff with meso-scale weather model rainfall estimates: a New Zealand experience. Journal of Hydrology 239, 19–32.

Jasper, K., Gurtz, J., Lang, H., 2002. Advanced flood forecasting in Alpine watersheds by coupling meteorological observations and forecasts with a distributed hydrological model. Journal of Hydrology 267, 40–52.

Kain, J.S., Fritsch, J.M., 1993. Convective parameterization for mesoscale models: The Kain e Fritsch (1993) scheme, The Representation of Cumulus Convection in Numerical Models. Meteorological Monographs American Meteorological Society 1993;, 165–170.

Kitanidis, P.K., Bras, R.L., 1980. Real time forecasting with a conceptual hydrologic model 2: applications and results. Water Resources Research 16 (6), 1034–1044.

Koussis, A.D., Lagouvardos, K., Mazi, K., Kotroni, V., Sitzmann, D., Lang, J., Zaiss, H., Buzzi, A., Malguzzi, P., 2003. Flood forecasts for urban basin with integrated hydro-meteorological model. Journal of Hydrologic Engineering 7, 1–11.

Lettenmaier, D.P., Wood, E.F., 1993. Hydrologic forecasting, in: Maidment, D.R. (Ed.), Handbook of Hydrology. McGraw-Hill, New York.

Liang, X., Lettenmaier, D.P., Wood, E.F., Burges, S.J., 1994. A simple hydrologically based model of land surface water and energy fluxes for general circulation models. Journal of Geophysical Research 99 (D7), 14415–14428.

Lin, Y., Farley, R.D., Orville, H.D., 1983. Bulk parameterisation of the snow field in a cloud model. Journal of Applied Meteorology 22, 1065–1092.

Mao, Q., Mueller, S.F., Juang, H.M.H., 2000. Quantitative precipitation forecasting for the Tennessee and Cumberland River watersheds using the NCEP regional spectral model. Weather and Forecasting 15, 29–45.

McBride, J.L., Ebert, E.E., 2000. Verification of quantitative precipitation forecasts from operational numerical weather prediction models over Australia. Weather and Forecasting 15, 103–121.

Mullen, S.L., Buizza, R., 2001. Quantitative precipitation forecasts over the United States by the ECMWF Ensemble Prediction System. Monthly Weather Review 129, 638–663.

NHWC, 2002. Use and benefits of the National Weather Service river and flood forecasts. National Hydrologic Warning Council, USA. 21 pp.

Nijssem, B., Lettenmaier, D.P., Liang, X., Wetzel, S.W., Wood, E.F., 1997. Streamflow simulation for continental-scale river basins. Water Resources Research 33 (4), 711–724.

Serban, P., Askew, A.J., 1991. Hydrological forecasting and updating procedures, In: Symposium Hydrology for the Water Management of Large River Basins (Proceedings of Symposium of the IAHS) 1991 pp. 357–369.

Tao, W.-K., Simpson, J., 1993. Goddard cumulus ensemble model. Part I. Model description. Terrestrial Atmospheric Ocean Science 4, 35–72.

Wood, E.F., Lettenmaier, D.P., Zartarian, V.G., 1992. A land surface hydrology parameterization with subgrid variability for general circulation models. Journal of Geophysical Research 97 (D3), 2717–2728.

Xue, M., Droegemeier, K.K., Wong, V., 2000. The advanced regional prediction system (ARPS): a multi-scale nonhydrostatic atmospheric simulation and prediction model. Part I. Model dynamics and verification. Meteorology and Atmospheric Physics 75, 161–193.

Xue, M., Wang, D.H., Gao, J.D., Brewster, K., Droegemeier, K.K., 2001. The advanced regional prediction system (ARPS): a multi-scale nonhydrostatic atmospheric simulation and prediction tool. Part II. Model physics and applications. Meteorology and Atmospheric Physics 76, 143–165.

Yapo, P.O., Gupta, H.V., Sorooshian, S., 1998. Multi-objective global optimization for hydrologic models. Journal of Hydrology 204, 83–97.

Yeh, W., Becker, L., Zettlemaoyer, R., 1982. Worth of inflow forecast for reservoir operation. Journal of Water Resources Planning and Management 108, 257–269.

Yu, Z., Lakhtakia, M.N., Yarnal, B., White, R.A., Miller, D.A., Frakes, B., Barron, E.J., Duffy, C., Schwartz, F.W., 1999. Simulating the river basin response to atmospheric forcing by linking a mesoscale meteorological model and hydrological model system. Journal of Hydrology 218, 72–91.